

Planetary Companions to Evolved Intermediate-Mass Stars: 14 Andromedae, 81 Ceti, 6 Lyncis, and HD 167042

Bun'ei SATO,¹ Eri TOYOTA,² Masashi OMIYA,³ Hideyuki IZUMIURA,^{4,5} Eiji KAMBE,⁴ Seiji MASUDA,⁶ Yoichi TAKEDA,^{5,7} Yoichi ITOH,² Hiroyasu ANDO,^{5,7} Michitoshi YOSHIDA,^{4,5} Eiichiro KOKUBO,^{5,7} and Shigeru IDA⁸

¹*Global Edge Institute, Tokyo Institute of Technology, 2-12-1-S6-6 Ookayama, Meguro-ku, Tokyo 152-8550*

sato.b.aa@m.titech.ac.jp

²*Graduate School of Science, Kobe University, 1-1 Rokkodai, Nada, Kobe 657-8501*

³*Department of Physics, Tokai University, 1117 Kitakaname, Hiratsuka, Kanagawa 259-1292*

⁴*Okayama Astrophysical Observatory, National Astronomical Observatory of Japan, Kamogata, Okayama 719-0232*

⁵*The Graduate University for Advanced Studies, Shonan Village, Hayama, Kanagawa 240-0193*

⁶*Tokushima Science Museum, Asutamu Land Tokushima, 45-22 Kibigadani, Nato, Itano-cho, Itano-gun, Tokushima 779-0111*

⁷*National Astronomical Observatory of Japan, 2-21-1 Osawa, Mitaka, Tokyo 181-8588*

⁸*Department of Earth and Planetary Sciences, Tokyo Institute of Technology, 2-12-1 Ookayama, Meguro-ku, Tokyo 152-8551*

(Received ; accepted)

Abstract

We report on the detection of four extrasolar planets orbiting evolved intermediate-mass stars from a precise Doppler survey of G–K giants at Okayama Astrophysical Observatory. All of the host stars are considered to be formerly early F-type or A-type dwarfs when they were on the main sequence. 14 And (K0 III) is a clump giant with a mass of $2.2 M_{\odot}$ and has a planet of minimum mass $m_2 \sin i = 4.8 M_J$ in a nearly circular orbit with a 186 day period. This is one of the innermost planets around evolved intermediate-mass stars and such planets have only been discovered in clump giants. 81 Cet (G5 III) is a clump giant with $2.4 M_{\odot}$ hosting a planet of $m_2 \sin i = 5.3 M_J$ in a 953 day orbit with an eccentricity of $e = 0.21$. 6 Lyn (K0 IV) is a less evolved subgiant with $1.7 M_{\odot}$ and has a planet of $m_2 \sin i = 2.4 M_J$ in a 899 day orbit with $e = 0.13$. HD 167042 (K1 IV) is also a less evolved star with $1.5 M_{\odot}$ hosting a planet of $m_2 \sin i = 1.6 M_J$ in a 418 day orbit with $e = 0.10$. This planet

was independently announced by Johnson et al. (2008, ApJ, 675, 784). All of the host stars have solar or sub-solar metallicity, which supports the lack of metal-rich tendency in planet-harboring giants in contrast to the case of dwarfs.

Key words: stars: individual: 14 And — stars: individual: 81 Cet — stars: individual: 6 Lyn — stars: individual: HD 167042 — planetary systems — techniques: radial velocities

1. Introduction

Precise Doppler surveys of evolved stars have opened a new frontier in extrasolar planet searches during the past several years. Since the successive discoveries of planets around K-type giants, ι Dra (Frink et al. 2002) and HD 47536 (Setiawan et al. 2003), and a G-type giant, HD 104985 (Sato et al. 2003), about 20 substellar companions orbiting evolved stars have been identified so far (Setiawan 2003; Setiawan et al. 2005; Sato et al. 2007, 2008; Hatzes et al. 2003, 2005, 2006; Reffert et al. 2006; Johnson et al. 2007, 2008; Lovis & Mayor 2007; Niedzielski et al. 2007; Döllinger et al. 2007; Liu et al. 2008). Planets in evolved stars is now one of the major subjects in the field of extrasolar planets.

In the past, planets around evolved stars were primarily studied from the interests in the fate of our solar system, that is, whether the Earth and the other planets will be engulfed by the Sun in the future (Sackmann et al. 1993; Duncan and Lissauer 1998). On the other hand, the current Doppler surveys of evolved stars have been mainly carried out in the context of planet searches around intermediate-mass ($1.5\text{--}5 M_{\odot}$) stars. Intermediate-mass stars on the main sequence, that is early-type dwarfs (B–A dwarfs), are more difficult for Doppler planet searches because they have fewer absorption lines in their spectra than later type ones, which are often broadened due to their rapid rotation, and thus it is more difficult to achieve a high measurement precision in radial velocity that is enough to detect orbiting planets (but see eg. Galland et al. 2005, 2006, which have developed a technique to extract Doppler information from spectra of A dwarfs sufficient for detection of substellar companions). This is actually one of the major reasons why targets for planet searches had been limited to low-mass ($< 1.5M_{\odot}$) F–M dwarfs. On the contrary, late G to early K giants and subgiants, which are intermediate-mass stars in evolved stages, have many sharp absorption lines in their spectra appropriate for precise radial velocity measurements and their surface activity such as pulsation is quiet enough not to prevent us from detecting planets. Therefore, these types of stars have been identified as promising targets for Doppler planet searches around intermediate-mass stars.

The ongoing planet searches have already revealed that the properties of planets around evolved intermediate-mass stars are probably different from those around low-mass dwarfs (see Bulter et al. 2006 or Udry and Santos 2007, and references therein for properties of planets around low-mass stars): 1) high frequency of massive planets (Lovis & Mayor 2007; Johnson et

al. 2007), which may be supported by the detection of a planet in an intermediate-mass giant in the Hyades open cluster (Sato et al. 2007) despite the absence of planets in low-mass hundred dwarfs in the cluster (Paulson et al. 2004), 2) lack of inner planets with orbital semimajor axes of $\lesssim 0.7$ AU (Johnson et al. 2007; Sato et al. 2008), and 3) lack of metal-rich tendency in the host stars of planets (Pasquini et al. 2007; Takeda et al. 2008). Although the properties must reflect history of formation and evolution of planetary systems dependent on their host stars' mass, they are still in need of confirmation by a larger number of samples. Combined with these observational progresses, planet formation theories applicable to more massive stars than the Sun have begun to develop rapidly (Ida and Lin 2005; Burkert and Ida 2007; Kennedy and Kenyon 2007) as extension of the standard theory for solar-mass ones (e.g., Hayashi et al. 1985; Ida and Lin 2004) for the first time since Nakano (1988) explored the idea nearly 20 years ago.

In this paper, we report on the detection of four planets orbiting intermediate-mass G–K giants and subgiants (14 And, 81 Cet, 6 Lyn, and HD 167042) from the Okayama Planet Search Program (Sato et al. 2005), one of which (HD 167042) was independently announced by Johnson et al. (2008, ApJ, 675, 784). We describe our observations in Section 2. Properties of the host stars, radial velocity data, and orbital parameters of their planets are presented in Section 3. Section 4 is devoted to an analysis of spectral line shape for the host stars. We summarize our results in Section 5 with a discussion about the properties of planets and host stars.

2. Observations

Since 2001, we have been conducting a precise Doppler survey of about 300 G–K giants (Sato et al. 2005) using a 1.88 m telescope, the HIgh Dispersion Echelle Spectrograph (HIDES; Izumiura 1999), and an iodine absorption cell (I₂ cell; Kambe et al. 2002) at Okayama Astrophysical Observatory (OAO). In 2007 December, HIDES was upgraded from single CCD (2K×4K) to a mosaic of three CCDs, which can simultaneously cover a wavelength range of 3750–7500Å using a RED cross-disperser (Izumiura et al. in preparation). For precise radial velocity measurements, we use a wavelength range of 5000–5800Å (covered by the middle CCD after the upgrade in 2007 December), in which many deep and sharp I₂ lines exist. A slit width is set to 200 μm (0.76") giving a spectral resolution ($R = \lambda/\Delta\lambda$) of 67000 by about 3.3 pixels sampling. We can typically obtain a signal-to-noise ratio $S/N > 200 \text{ pix}^{-1}$ for a $V < 6.5$ star with an exposure time shorter than 30 min. We have achieved a long-term Doppler precision of about 6 m s⁻¹ over a time span of 7 years using our own analysis software for modeling an I₂-superposed stellar spectrum (Sato et al. 2002, 2005). Recently, we have succeeded in attaining a Doppler precision of about 2 m s⁻¹ in week-long time scale by improving the analysis software (Kambe et al. 2008). We are now trying to maintain the same precision in year-long time scale.

For abundance analysis, we take a pure (I₂-free) stellar spectrum with the same wave-

length range and spectral resolution as those for radial velocity measurements. We also take a spectrum covering Ca II H K lines in order to check the chromospheric activity for stars showing large radial velocity variations. Although we can take the spectrum simultaneously with radial velocity data after the upgrade of HIDES, the spectra presented in this paper except for HD 167042 were obtained before the upgrade. In that case, we set the wavelength range to 3800–4500 Å using a BLUE cross-disperser and the slit width to 250 μm giving a wavelength resolution of 50000. We typically obtained S/N $\simeq 20 \text{ pix}^{-1}$ at the Ca II H K line cores for a $B = 6$ star with a 30 min exposure.

The reduction of echelle data (i.e. bias subtraction, flat-fielding, scattered-light subtraction, and spectrum extraction) is performed using the IRAF¹ software package in the standard way.

3. Stellar Properties, Radial Velocities, and Orbital Solutions

3.1. 14 Andromedae

14 And (HR 8930, HD 221345, HIP 116076) is listed in the Hipparcos catalog (ESA 1997) as a K0 III giant star with a V magnitude $V = 5.22$ and a color index $B - V = 1.029$. The Hipparcos parallax $\pi = 13.09 \pm 0.71$ mas corresponds to a distance of 76.4 ± 4.1 pc and an absolute magnitude $M_V = 0.67$ taking account of correction of interstellar extinction $A_V = 0.13$ based on the Arenou et al’s (1992) table. *Hipparcos* made a total of 80 observations of the star, revealing a photometric stability down to $\sigma = 0.006$ mag. Ca II H K lines of the star show no significant emission in the line cores as shown in the Figure 1, suggesting that the star is chromospherically inactive.

We derived atmospheric parameters and Fe abundance of ~ 320 G–K giants including all targets for the Okayama Planet Search Program based on the spectroscopic approach using the equivalent widths of well-behaved Fe I and Fe II lines (cf. Takeda et al. 2002 for a detailed description of this method; Takeda et al. 2008). For 14 And, $T_{\text{eff}} = 4813$ K, $\log g = 2.63$ cm s⁻², $v_t = 1.43$ km s⁻¹, and $[\text{Fe}/\text{H}] = -0.24$ were obtained. The bolometric correction was estimated to $B.C. = -0.33$ based on the Kurucz (1993)’s theoretical calculation. With use of these parameters and theoretical evolutionary tracks of Lejeune & Schaerer (2001), we obtained the fundamental stellar parameters, $L = 58L_{\odot}$, $R = 11R_{\odot}$, and $M = 2.2M_{\odot}$, as summarized in Table 1. The procedure described here is the same as that adopted in Takeda et al. (2005) (see subsection 3.2 of Takeda et al. (2005) and Note of Table 1 for uncertainties involved in the stellar parameters). The projected rotational velocity $v \sin i = 2.60$ km s⁻¹ was also obtained by Takeda et al. (2008). Mishenina et al. (2006) obtained $T_{\text{eff}} = 4664$ K (from line-

¹ IRAF is distributed by the National Optical Astronomy Observatories, which is operated by the Association of Universities for Research in Astronomy, Inc. under cooperative agreement with the National Science Foundation, USA.

depth-ratio analysis), $\log g = 2.20 \text{ cm s}^{-2}$, $v_t = 1.4 \text{ km s}^{-1}$, $[\text{Fe}/\text{H}] = -0.37$, and $M = 1.5M_\odot$ for the star. The temperature and $[\text{Fe}/\text{H}]$ are by $\sim 150 \text{ K}$ and by $\sim 0.1 \text{ dex}$ lower than our estimates, respectively. Such differences can produce $\sim 0.5M_\odot$ difference in mass of a clump giant especially for metal-poor case depending on evolutionary models (see Note of Table 1). As shown in Figure 2, the star is located at the clump region on the HR diagram.

We collected a total of 34 radial velocity data of 14 And between 2004 January and 2008 January, with a typical S/N of 200 pix^{-1} for an exposure time of about 600 s. The observed radial velocities are shown in Figure 3 and are listed in Table 2 together with their estimated uncertainties, which were derived from an ensemble of velocities from each of ~ 200 spectral regions (each $4\text{--}5\text{\AA}$ long) in every exposure. Lomb-Scargle periodogram (Scargle 1982) of the data exhibits a dominant peak at a period of 188 days. To assess the significance of this periodicity, we estimated False Alarm Probability (*FAP*), using a bootstrap randomization method in which the observed radial velocities were randomly redistributed, keeping fixed the observation time. We generated 10^5 fake datasets in this way, and applied the same periodogram analysis to them. Since no fake datasets exhibited a periodogram power higher than the observed dataset, the *FAP* is less than 1×10^{-5} .

The observed radial velocities can be well fitted by a circular orbit with a period $P = 185.84 \pm 0.23$ days and a velocity semiamplitude $K_1 = 100.0 \pm 1.3 \text{ m s}^{-1}$. The resulting model is shown in Figure 3 overplotted on the velocities, and its parameters are listed in Table 3. The uncertainty of each parameter was estimated using a Monte Carlo approach. We generated 300 fake datasets by adding random Gaussian noise corresponding to velocity measurement errors to the observed radial velocities in each set, then found the best-fit Keplerian parameters for each, and examined the distribution of each of the parameters. The rms scatter of the residuals to the Keplerian fit was 20.3 m s^{-1} , which is comparable to the scatters of giants with the same $B - V$ as 14 And in our sample (Sato et al. 2005). Adopting a stellar mass of $2.2 M_\odot$, we obtain a minimum mass for the companion of $m_2 \sin i = 4.8M_J$ and a semimajor axis of $a = 0.83 \text{ AU}$. The planet is one of the innermost planets ever discovered around evolved stars.

3.2. 81 Ceti

81 Ceti (HR 771, HD 16400, HIP 12247) is listed in the Hipparcos catalog (ESA 1997) as a G5 III: giant star with a V magnitude $V = 5.65$, a color index $B - V = 1.021$, and a parallax $\pi = 10.29 \pm 0.97 \text{ mas}$, corresponding to a distance of $97.2 \pm 9.2 \text{ pc}$ and an absolute magnitude $M_V = 0.63$ corrected by interstellar extinction $A_V = 0.08$ (Arenou et al. 1992). *Hipparcos* made a total of 58 observations of the star, revealing a photometric stability down to $\sigma = 0.006 \text{ mag}$. Ca II H K lines of the star show no significant emission in the line cores as shown in the Figure 1, suggesting that the star is chromospherically inactive. We derived fundamental stellar parameters for the star of $T_{\text{eff}} = 4785 \text{ K}$, $\log g = 2.35 \text{ cm s}^{-2}$, $v_t = 1.33 \text{ km s}^{-1}$, $[\text{Fe}/\text{H}] = -0.06$, $L = 60L_\odot$, $R = 11R_\odot$, and $M = 2.4M_\odot$, as summarized in Table 1. As shown in Figure

2, the star is located at the clump region on the HR diagram. Mishenina et al. (2006) derived $T_{\text{eff}} = 4840$ K (from line-depth-ratio analysis), $\log g = 2.50$ cm s⁻², $v_t = 1.35$ km s⁻¹, $[\text{Fe}/\text{H}] = -0.01$, and $M = 2.5M_{\odot}$ for the star, which reasonably agree with our estimates.

We collected a total of 33 radial velocity data of 81 Cet between 2003 September and 2008 March, with a typical S/N of 200 pix⁻¹ for an exposure time of 900 s. The observed radial velocities are shown in Figure 4 and are listed in Table 4 together with their estimated uncertainties. Lomb-Scargle periodogram (Scargle 1982) of the data exhibits a dominant peak at a period of 983 days with a $FAP < 1 \times 10^{-5}$, which is estimated by the same way as described in Section 3.1.

The observed radial velocities can be well fitted by a Keplerian orbit with a period $P = 952.7 \pm 8.8$ days, a velocity semiamplitude $K_1 = 62.8 \pm 1.5$ m s⁻¹, and an eccentricity $e = 0.206 \pm 0.029$. The resulting model is shown in Figure 4 overplotted on the velocities, and its parameters are listed in Table 3. The uncertainty of each parameter was estimated using a Monte Carlo approach as described in Section 3.1. The rms scatter of the residuals to the Keplerian fit is 9.2 m s⁻¹, which is small compared to the typical scatters of giants with the same $B - V$ as 81 Cet in our sample (Sato et al. 2005). Adopting a stellar mass of $2.4 M_{\odot}$, we obtain a minimum mass for the companion $m_2 \sin i = 5.3M_J$ and a semimajor axis $a = 2.5$ AU. The planet is one of the outermost planets ever discovered around evolved stars.

3.3. 6 Lyncis

6 Lyn (HR 2331, HD 45410, HIP 31039) is a less evolved K0 subgiant star with a V magnitude $V = 5.86$, a color index $B - V = 0.934$, and the Hipparcos parallax $\pi = 17.56 \pm 0.76$ mas (ESA 1997), placing the star at a distance of 56.9 ± 2.5 pc. The distance and an estimated interstellar extinction $A_V = 0.03$ (Arenou et al. 1992) yield an absolute magnitude for the star $M_V = 2.05$. *Hipparcos* made a total of 73 observations of the star, revealing a photometric stability down to $\sigma = 0.005$ mag. Ca II H K lines of the star show no significant emission in the line cores as shown in the Figure 1, suggesting that the star is chromospherically inactive. We derived fundamental stellar parameters for the star of $T_{\text{eff}} = 4978$ K, $\log g = 3.16$ cm s⁻², $v_t = 1.10$ km s⁻¹, $[\text{Fe}/\text{H}] = -0.13$, $L = 15L_{\odot}$, $R = 5.2R_{\odot}$, and $M = 1.7M_{\odot}$, as summarized in Table 1. The position of the star on the HR diagram is plotted in Figure 2 based on these parameters.

We collected a total of 30 radial velocity data of 6 Lyn between 2004 January and 2008 March, with a typical S/N of 200 pix⁻¹ for an exposure time of about 1200 s. The observed radial velocities are shown in Figure 5 and are listed in Table 5 together with their estimated uncertainties. Lomb-Scargle periodogram (Scargle 1982) of the data exhibits a dominant peak at a period of 917 days with a $FAP < 1 \times 10^{-5}$, which is estimated by the same way as described in Section 3.1.

The observed radial velocities can be well fitted by a Keplerian orbit with a period

$P = 899 \pm 19$ days, a velocity semiamplitude $K_1 = 36.2 \pm 1.7$ m s⁻¹, and an eccentricity $e = 0.134 \pm 0.052$. The resulting model is shown in Figure 5, and its parameters are listed in Table 3. The uncertainty of each parameter was estimated using a Monte Carlo approach as described in Section 3.1. The rms scatter of the residuals to the Keplerian fit was 10.6 m s⁻¹, which is comparable to those for subgiants (Johnson et al. 2007). Adopting a stellar mass of $1.7 M_\odot$, we obtain a minimum mass for the companion of $m_2 \sin i = 2.4 M_J$ and a semimajor axis of $a = 2.2$ AU.

3.4. HD 167042

HD 167042 (HR 6817, HIP 89047) is classified in the Hipparcos catalog (ESA 1997) as a K1 III star with a V magnitude $V = 5.97$ and a color index $B - V = 0.943$. The Hipparcos parallax $\pi = 20.00 \pm 0.51$ mas corresponds to a distance of 50.0 ± 1.3 pc and yields an absolute magnitude $M_V = 2.47$ corrected by interstellar extinction $A_V = 0.01$ (Arenou et al. 1992). *Hipparcos* made a total of 110 observations of the star, revealing a photometric stability down to $\sigma = 0.007$ mag. Ca II H K lines of the star show no significant emission in the line cores, suggesting that the star is chromospherically inactive (Figure 1). We derived fundamental stellar parameters for the star of $T_{\text{eff}} = 4943$ K, $\log g = 3.28$ cm s⁻², $v_t = 1.07$ km s⁻¹, $[\text{Fe}/\text{H}] = +0.00$, $L = 10L_\odot$, $R = 4.5R_\odot$, and $M = 1.5M_\odot$, as summarized in Table 1. The position of the star on the HR diagram is plotted in Figure 2 based on these parameters. Judged from the position, the star is considered to be a less evolved subgiant like 6 Lyn rather than a class III giant. Johnson et al. (2008) obtained $T_{\text{eff}} = 5010 \pm 75$ K, $\log g = 3.47 \pm 0.08$ cm s⁻², $[\text{Fe}/\text{H}] = +0.05 \pm 0.06$, $M = 1.64 \pm 0.13M_\odot$, $R = 4.30 \pm 0.07R_\odot$, and $L = 10.5 \pm 0.05L_\odot$ for the star, all of which we agree with our estimates within the errors.

A planetary companion to HD 167042 was recently reported by Johnson et al. (2008). We collected a total of 29 radial velocity data of the star between 2004 March and 2008 March, which is almost the same period of time as that of Johnson et al. The data have typical S/N of 200 pix⁻¹ for exposure time of about 1500 s. The observed radial velocities are shown in Figure 6 and are listed in Table 6 together with their estimated uncertainties. Lomb-Scargle periodogram (Scargle 1982) of the data exhibits a dominant peak at a period of 432 days with a $FAP < 1 \times 10^{-5}$, which is estimated by the same way as described in Section 3.1.

The observed radial velocities can be well fitted by a Keplerian orbit with a period $P = 417.6 \pm 4.5$ days, a velocity semiamplitude $K_1 = 33.3 \pm 1.6$ m s⁻¹, and an eccentricity $e = 0.101 \pm 0.066$. The resulting model is shown in Figure 6, and its parameters are listed in Table 3. The uncertainty of each parameter was estimated using a Monte Carlo approach as described in Section 3.1. The rms scatter of the residuals to the Keplerian fit was 8.0 m s⁻¹, which is consistent with Johnson et al. (2008)'s result. Adopting a stellar mass of $1.5 M_\odot$, we obtain a minimum mass for the companion of $m_2 \sin i = 1.6 M_J$ and a semimajor axis of $a = 1.3$ AU. All of the parameters are in good agreement with those obtained by Johnson et al. (2008)

and thus we have independently confirmed the existence of the planet.

4. Line Shape Analysis

To investigate other causes producing apparent radial velocity variations such as pulsation and rotational modulation rather than orbital motion, spectral line shape analysis was performed with use of high resolution stellar templates followed by the technique of Sato et al. (2007). In our technique, we extract a high resolution iodine-free stellar template from several stellar spectra contaminated by iodine lines (Sato et al. 2002). Basic procedure of the technique is as follows; first, we model observed star+I₂ spectrum in a standard manner but using the initial guess of the intrinsic stellar template spectrum. Next we take the difference between the observed star+I₂ spectrum and the modeled one. Since the difference is mainly considered to be due to an imperfection of the initial guess of the stellar template spectrum, we revise the initial guess taking account of the difference and model the observed star+I₂ spectrum using the revised guess of the template. We repeat this process until we obtain sufficient agreement between observed and modeled spectrum. We take average of thus obtained stellar templates from several observed star+I₂ spectra to increase S/N ratio of the template. Details of this technique are described in Sato et al. (2002).

For spectral line shape analysis, we extracted two stellar templates from 5 star+I₂ spectra at the peak and valley phases of observed radial velocities for each star. Then, cross correlation profiles of the two templates were calculated for 50–80 spectral segments (4–5Å width each) in which severely blended lines or broad lines were not included. Three bisector quantities were calculated for the cross correlation profile of each segment: the velocity span (BVS), which is the velocity difference between two flux levels of the bisector; the velocity curvature (BVC), which is the difference of the velocity span of the upper half and lower half of the bisector; and the velocity displacement (BVD), which is the average of the bisector at three different flux levels. We used flux levels of 25%, 50%, and 75% of the cross correlation profile to calculate the above quantities. Resulting bisector quantities for each star are listed in Table 7. As expected from the planetary hypothesis, both of the BVS and the BVC for 81 Cet, 6 Lyn, and HD 167042 are identical to zero, which means that the cross correlation profiles are symmetric, and the average BVD is consistent with the velocity difference between the two templates at the peak and valley phases of observed radial velocities ($\simeq 2K_1$). The BVS for 14 And is about 20 m s⁻¹, which is large compared to those for other stars, suggesting the higher intrinsic variability and possible variations in the line profiles for the star. This may be consistent with the large rms scatters of the residuals to the Keplerian fit ($\sigma = 20.3$ m s⁻¹) and higher rotational velocity ($v \sin i = 2.6$ km s⁻¹) for the star. However, the BVD value (-177 m s⁻¹) is consistent with the velocity difference between the two templates ($\simeq 2K_1$) and the BVS value is only about one ninth of the BVD. Thus it is unlikely that the observed radial velocity variations are produced by changes in the line shape due to intrinsic activity such as pulsation or rotational modulation.

Based on these results, we conclude that the radial velocity variability observed in these 4 stars are best explained by orbital motion, although line shape variability for 14 And deserves to be investigated in more detail.

5. Summary and Discussion

We here reported four new planets around evolved intermediate-mass stars from the Okayama Planet Search Program; two of them orbit clump giants and the other two orbit subgiants. In total, we discovered 7 planets and 1 brown dwarf around intermediate-mass clump giants ($2.1\text{--}2.7M_{\odot}$) and 2 planets around subgiants (1.5 and $1.7M_{\odot}$) so far from the program. The host stars are considered to be formerly early F-type or A-type dwarfs when they were on the main sequence.

Like all of the other planets found around these types of stars, the four planets presented in this paper reside beyond ~ 0.7 AU from the central stars. Since many planets are known to exist within 0.7 AU around low-mass dwarfs, the lack of inner planets around evolved intermediate-mass stars must reflect different history of formation and evolution of planetary systems. Two scenarios can account for the orbital distribution; one is that inner planets are primordially deficient around intermediate-mass stars and the other is that they have been engulfed by the expanding central stars due to stellar evolution. Mass loss of the central star makes planets move outward because of their weakened gravitational pull on the planets, but orbital change due to mass loss is negligible in RGB phase for planets around intermediate-mass stars because the mass loss of those stars in RGB phase is negligible (see discussion in Sato et al. 2008). The lack of inner planets around less evolved subgiants (Johnson et al. 2007, 2008) may favor the former scenario. Since there is no observational bias against detecting planets with small semimajor axes around subgiants, whose radii are $\sim 5R_{\odot}$ ($= 0.025$ AU) at most and their intrinsic variability in radial velocity is adequately small ($\lesssim 10$ m s $^{-1}$), the lack of inner planets around them may be primordial. On the other hand, as for planets around intermediate-mass clump giants, evolutionary effect of the central stars can not be ignored. When we assume that many of clump giants are post-RGB stars (core-helium-burning stars), planets in orbits with $\lesssim 0.5$ AU could have been engulfed by the central stars at the tip of RGB ($R_{\star} \sim 25\text{--}40R_{\odot}$ for a $2\text{--}3 M_{\odot}$ star) due to tidal force from the central stars (Sato et al. 2008). Thus we can not reject the possibility that planets had originally existed in short orbital distances around progenitors of clump giants. It should be noted that all of the four innermost planets around evolved intermediate-mass stars with semimajor axes of $0.7\text{--}1$ AU have been discovered around clump giants. Excluding the planets around clump giants, all of the six planets ever discovered around intermediate-mass subgiants reside beyond 1 AU, which expands the lack of inner planets around them. Although the number is still small, properties of planets might be different between the two populations when we consider that clump giants include $\gtrsim 2M_{\odot}$ stars while subgiants are limited up to $\lesssim 2M_{\odot}$. Larger number of planets, which

will be provided by ongoing Doppler surveys of evolved stars among the globe, enables us to derive their statistical properties more clearly.

All of the host stars of the four planets presented here have solar or sub-solar metallicity. The results support the lack of metal-rich tendency in planet-harboring giants recently claimed by several authors (e.g., Pasquini et al. 2007; Takeda et al. 2008), which makes marked contrast to the case of dwarf stars, where planet-harboring stars tend to be generally metal-rich (see e.g., Gonzalez 2003 or Udry and Santos 2007, and references therein). Interpretation of the absence of metal-rich trend in planet-harboring giants still remains to be cleared. High efficiency in core-accretion in massive proto-planetary disks around massive stars combined with high efficiency in inward orbital migration of planets (finally falling into the central stars) in metal-rich disks might reproduce the lack of metal-rich trend. Alternatively, metallicity-independent planet formation scenario such as disk instability model (e.g., Boss 2002) might be possible. Pasquini et al. (2007) pointed out a possibility that metallicity excess in planet-harboring dwarfs originates from accretion of metal-rich material and the excess is diluted by deep convective envelope at the stage of giants. It should be noted, however, that there are no super-metal-rich stars with $[\text{Fe}/\text{H}] > +0.2$ in our sample regardless of the existence of orbiting planets (Takeda et al. 2008). Since the frequency distribution of planets steeply rises in $[\text{Fe}/\text{H}] > +0.2$ for solar-type dwarfs (Fischer & Valenti 2005), we might see metal-poor ($[\text{Fe}/\text{H}] < +0.2$) tail of the same distribution, where frequency of planets is less sensitive to metallicity, in the case of giants. Detailed investigation of metallicity distribution for a population of giants is required to derive a firm conclusion on planet-metallicity correlation in giants and its origin.

Host stars' metallicity could control the fate of orbiting planets as well as their birth. From the view point of the engulfment scenario, inner planets could be deficient around metal-rich clump giants of $\sim 2M_{\odot}$ compared to around metal-poor ones. A metal-rich star with $\sim 2M_{\odot}$ can have more than two times larger maximum radius ($> 70R_{\odot}$) than a metal-poor one at the tip of RGB (cf. evolutionary tracks by Girardi et al. 2000; Lejeune and Schaerer 2001; Claret 2004, 2006, 2007), which may increase a chance for the central star to engulf inner planets even up to ~ 1 AU. However, the current knowledge about evolutionary tracks of giants is not sufficient to estimate this effect precisely. Stellar evolutionary track at RGB phase for a $\sim 2M_{\odot}$ star is sensitive to slight difference in stellar mass and metallicity because this mass range is a border where helium burning starts in a degenerated core or a non-degenerated one and thus the tracks are largely dependent on adopted models. To investigate orbital distribution of planets around post-RGB stars together with precise determination of stellar mass (by using technique of asteroseismology; e.g., Frandsen et al. 2002; Hatzes & Zechmeister 2007; Ando et al. 2008) and metallicity would conversely give constraints on stellar evolution for this problematic mass range from observational side.

As described above, the recent discoveries of planets around evolved stars have made stellar evolution and fate of planets a renewed area of study. This subject has been studied

by several authors (Sackmann et al. 1993; Duncan and Lissauer 1998; Rasio et al. 1996; Siess and Livio 1999ab; Villanver and Livio 2007) mainly focusing on a solar-mass star based on the interests in the future of the solar system, and/or an asymptotic giant branch star with the scope of planets in planetary nebula and white dwarfs. Siess and Livio (1999b) proposed that the IR excess and high Li abundance observed in a few percent of G–K giants originate from the accretion of a substellar companion. Now is the time to promote such kinds of studies more extensively not only for solar-mass stars but also for intermediate-mass ones especially in RGB phase by both theoretical and observational approaches.

This research is based on data collected at Okayama Astrophysical Observatory (OAO), which is operated by National Astronomical Observatory of Japan (NAOJ). We are grateful to all the staff members of OAO for their support during the observations. Data analysis was in part carried out on “sb” computer system operated by the Astronomy Data Center (ADC) and Subaru Telescope of NAOJ. We thank the National Institute of Information and Communications Technology for their support on high-speed network connection for data transfer and analysis. B.S. is supported by MEXT’s program “Promotion of Environmental Improvement for Independence of Young Researchers” under the Special Coordination Funds for Promoting Science and Technology. H.I. and M.Y. are supported by Grant-in-Aid for Scientific Research (C) No.13640247 and (B) No.18340055, respectively, from the Japan Society for the Promotion of Science (JSPS). This research has made use of the SIMBAD database, operated at CDS, Strasbourg, France.

References

- Ando, H., Tan, K., Kambe, E., Sato, B., & Zhao, G. 2008, PASJ, 60, 219
Arenou, F., Grenon, M., & Gomez, A. 1992, A&A, 258, 104
Boss, A.P. 2002, ApJ, 567, L149
Burkert, A., & Ida, S. 2007, ApJ, 660, 845
Butler, R.P., et al. 2006, ApJ, 646, 505
Claret, A. 2007, A&A, 467, 1389
Claret, A. 2006, A&A, 453, 769
Claret, A. 2004, A&A, 424, 919
Döllinger, M.P., Hatzes, A.P., Pasquini, L., Guenther, E.W., Hartmann, M., Girardi, L., & Esposito, M. 2007, A&A, 472, 649
Duncan, M.J., & Lissauer, J.J. 1998, Icarus, 134, 303
ESA. 1997, The *Hipparcos* and *Tycho* Catalogues (ESA SP-1200; Noordwijk: ESA) A&A, 394, 5
Fischer, D.A. & Valenti, J. 2005, ApJ, 622, 1102
Frink, S., Mitchell, D.S., Quirrenbach, A., Fischer, D., Marcy, G.W., & Butler, R.P. 2002, ApJ, 576, 478

- Galland, F., Lagrange, A.-M., Udry, S., Chelli, A., Pepe, F., Beuzit, J.-L., & Mayor, M. 2005, *A&A*, 444, L21
- Galland, F., Lagrange, A.-M., Udry, S., Beuzit, J.-L., Pepe, F., & Mayor, M. 2006, *A&A*, 452, 709
- Girardi, L., Bressan, A., Bertelli, G., & Chiosi, C. 2000, *A&AS*, 141, 371
- Gonzalez, G. 2003, *Rev. Mod. Phys.*, 75, 101
- Hatzes, A.P., et al. 2003, *ApJ*, 599, 1383
- Hatzes, A.P., Guenther, E.W., Endl, M., Cochran, W.D., Döllinger, M.P., & Bedalov, A. 2005, *A&A*, 437, 743
- Hatzes, A.P., et al. 2006, *A&A*, 457, 335
- Hatzes, A.P., & Zechmeister, M. 2007, *ApJ*, 670, L37
- Hayashi, C., Nakazawa, K., & Nakagawa, Y. 1985, in *Protostars and planets II* (A86-12626 03-90). Tucson, AZ, University of Arizona Press, p. 1100-1153
- Ida, S., & Lin, D.N.C. 2004, *ApJ*, 604, 388
- Ida, S., & Lin, D.N.C. 2005, *ApJ*, 626, 1045
- Izumiura, H. 1999, in *Proc. 4th East Asian Meeting on Astronomy*, ed. P.S. Chen (Kunming: Yunnan Observatory), 77
- Johnson, J.A., et al. 2007, *ApJ*, 665, 785
- Johnson, J.A., et al. 2008, *ApJ*, 675, 784
- Kambe, E., et al. 2002, *PASJ*, 54, 865
- Kambe, E., et al. 2008, *PASJ*, 60, 45
- Kennedy, G.M. and Kenyon, S.J. 2008, *ApJ*, 673, 502
- Kurucz, R. L. 1993, Kurucz CD-ROM, No. 13 (Harvard-Smithsonian Center for Astrophysics)
- Lejeune, T., & Schaerer, D. 2001, *A&A*, 366, 538
- Liu, Y.-J., et al. 2008, *ApJ*, 672, 553
- Lovis, C., & Mayor, M. 2007, *A&A*, 472, 657
- Mishenina, T.V., et al. 2006, *A&A*, 456, 1109
- Nakano, T. 1988, *MNRAS*, 230, 551
- Niedzielski, A., et al. 2007, *ApJ*, 669, 1354
- Pasquini, L., et al. 2007, *A&A*, 473, 979
- Paulson, D.B., Cochran, W.D., & Hatzes, A.P. 2004, *AJ*, 127, 3579
- Rasio, F.A., Tout, C.A., Lubow, S.H., & Livio, M. 1996, *ApJ*, 470, 1187
- Reffert, S., et al. 2006, *ApJ*, 652, 661
- Sackmann, I.J., Boothroyd, A.I., & Kraemer, K.E. 1993, *ApJ*, 418, 457
- Sato, B., et al. 2003, *ApJ*, 597, L157
- Sato, B., Kambe, E., Takeda, Y., Izumiura, H., & Ando, H. 2002, *PASJ*, 54, 873
- Sato, B., Kambe, E., Takeda, Y., Izumiura, H., Masuda, S., & Ando, H. 2005, *PASJ*, 57, 97
- Sato, B., et al. 2007, *ApJ*, 661, 527
- Sato, B., et al. 2008, *PASJ*, in press
- Scargle, J. D. 1982, *ApJ*, 263, 835
- Setiawan, J., et al. 2003, *A&A*, 398, L19

- Setiawan, J. DARWIN/TPF and the Search for Extrasolar Terrestrial Planets, 22-25 April 2003, Heidelberg, Germany. Edited by M. Fridlund, T. Henning, compiled by H. Lacoste. ESA SP-539, Noordwijk, Netherlands: ESA Publications Division, 2003, p. 595-598
- Setiawan, J., et al. 2005, A&A, 437, 31
- Siess, L., & Livio, M. 1999a, MNRAS, 304, 925
- Siess, L., & Livio, M. 1999b, MNRAS, 308, 1133
- Takeda, Y., Ohkubo, M., & Sadakane, K. 2002, PASJ, 54, 451
- Takeda, Y., Sato, B., Kambe, E., Izumiura, H., Masuda, S., & Ando, H. 2005, PASJ, 57, 109
- Takeda, Y., Sato, B., & Murata, D. 2008, PASJ in press
- Udry, S. & Santos, N.C. 2007, ARA&A, 45, 397
- Villaver, E., & Livio, M. 2007, ApJ, 661, 1192

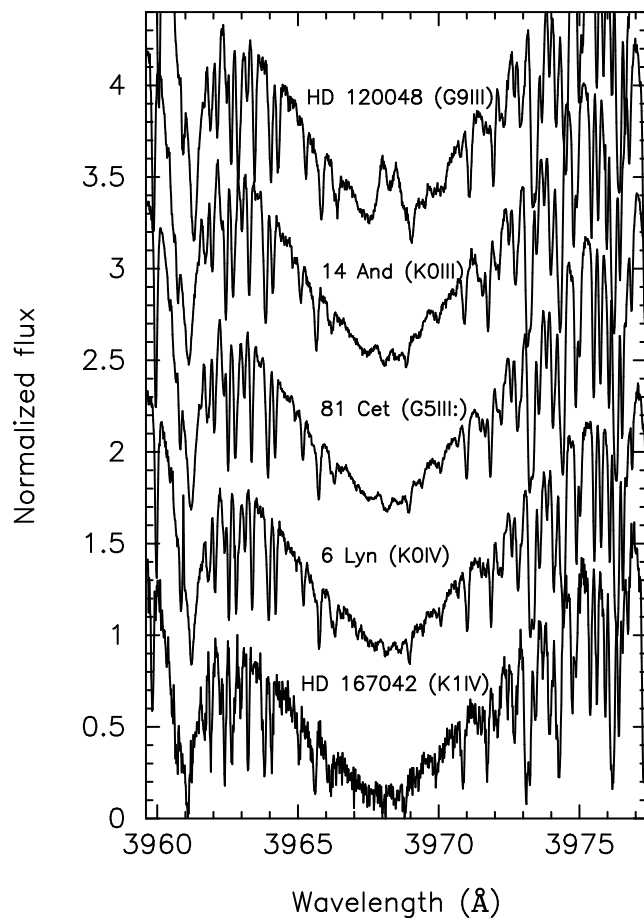


Fig. 1. Spectra in the region of Ca H lines. All of the planet-harboring stars show no significant emissions in line cores compared to that in the chromospheric active star HD 120048, which exhibits velocity scatter of about 30 m s^{-1} . A vertical offset of about 0.7 is added to each spectrum.

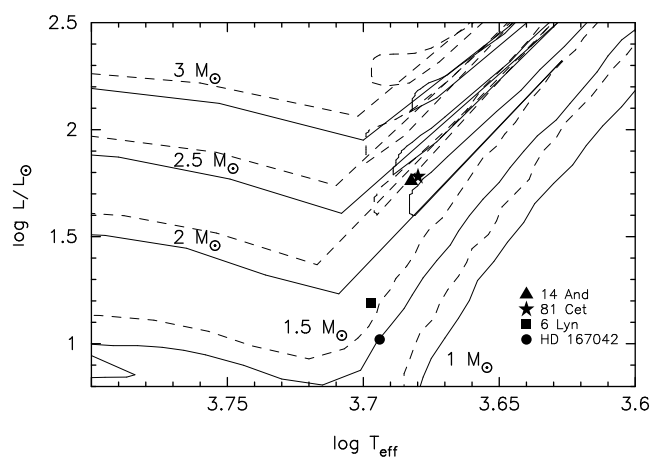


Fig. 2. HR diagram of the planet-harboring stars presented in this paper. Pairs of evolutionary tracks from Lejeune and Schaerer (2001) for stars with $Z = 0.02$ (solar metallicity; solid lines) and $Z = 0.008$ (dashed lines) of masses between 1 and $3 M_{\odot}$ are also shown.

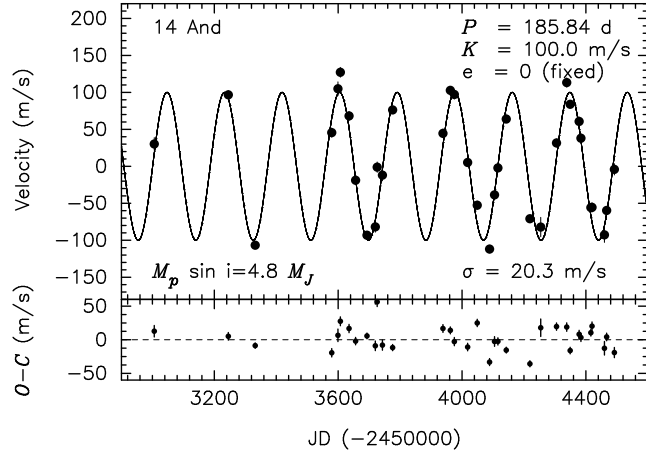


Fig. 3. *Top:* Observed radial velocities of 14 And (dots). The Keplerian orbital fit is shown by the solid line. *Bottom:* Residuals to the Keplerian fit. The rms to the fit is 20.3 m s^{-1} .

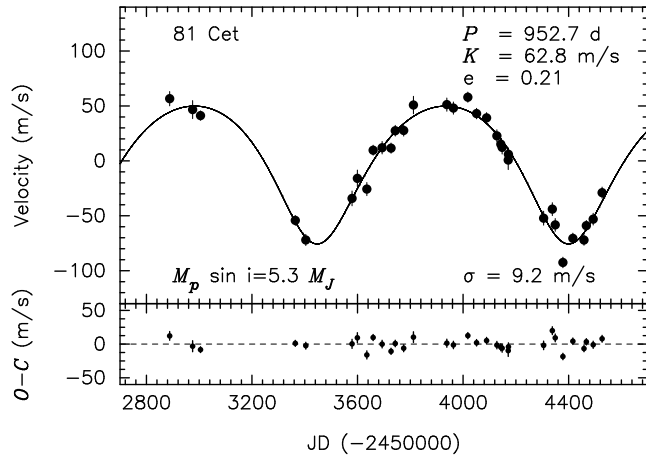


Fig. 4. *Top:* Observed radial velocities of 81 Cet (dots). The Keplerian orbital fit is shown by the solid line. *Bottom:* Residuals to the Keplerian fit. The rms to the fit is 9.2 m s^{-1} .

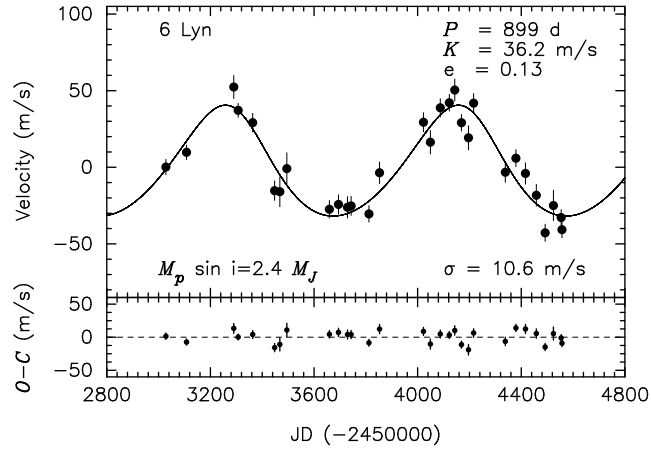


Fig. 5. *Top:* Observed radial velocities of 6 Lyn (dots). The Keplerian orbital fit is shown by the solid line. *Bottom:* Residuals to the Keplerian fit. The rms to the fit is 10.6 m s^{-1} .

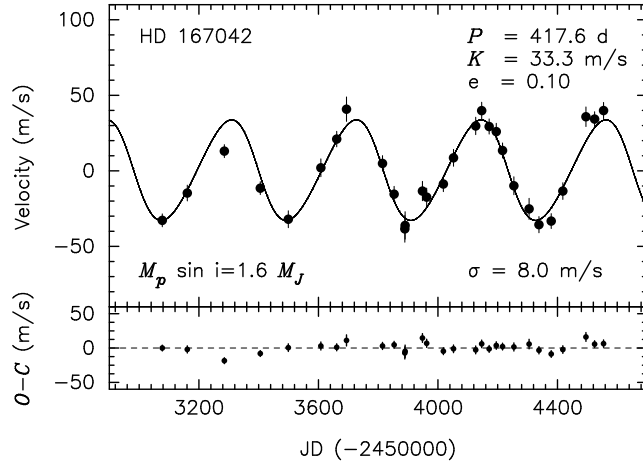


Fig. 6. *Top:* Observed radial velocities of HD 167042 (dots). The Keplerian orbital fit is shown by the solid line. *Bottom:* Residuals to the Keplerian fit. The rms to the fit is 8.0 m s^{-1} .

Table 1. Stellar parameters

Parameter	14 And	81 Cet	6 Lyn	HD 167042
Sp. Type	K0 III	G5 III:	K0 IV	[†] K1 IV
π (mas)	13.09±0.71	10.29±0.97	17.56±0.76	20.00±0.51
V	5.22	5.65	5.86	5.97
$B - V$	1.029	1.021	0.934	0.943
A_V	0.13	0.08	0.03	0.01
M_V	0.67	0.63	2.05	2.47
$B.C.$	-0.33	-0.34	-0.27	-0.28
T_{eff} (K)	4813±20	4785±25	4978±18	4943±12
$\log g$	2.63±0.07	2.35±0.08	3.16±0.05	3.28±0.05
v_t	1.43±0.09	1.33±0.06	1.10±0.07	1.07±0.07
[Fe/H]	-0.24±0.03	-0.06±0.03	-0.13±0.02	+0.00±0.02
L (L_{\odot})	58	60	15	10
R (R_{\odot})	11 (10–12)	11 (10–13)	5.2 (4.9–5.6)	4.5 (4.3–4.7)
M (M_{\odot})	2.2 (2.0–2.3)	2.4 (2.0–2.5)	1.7 (1.5–1.8)	1.5 (1.3–1.7)
$v \sin i$ (km s ⁻¹)	2.60	1.80	1.32	0.67

[†] The star is listed in the Hipparcos catalogue as a K1 III giant. But judged from the position of the star on the HR diagram (Figure 2), the star should be better classified as a less evolved subgiant.

Note – The uncertainties of [Fe/H], T_{eff} , $\log g$, and v_t , are internal statistical errors (for a given data set of Fe I and Fe II line equivalent widths) evaluated by the procedure described in subsection 5.2 of Takeda et al. (2002). Since these parameter values are sensitive to slight changes in the equivalent widths as well as to the adopted set of lines (Takeda et al. 2008), realistic ambiguities may be by a factor of ~ 2 –3 larger than these estimates from a conservative point of view (e.g., 50–100 K in T_{eff} , 0.1–0.2 dex in $\log g$). Values in the parenthesis for stellar radius and mass correspond to the range of the values assuming the realistic uncertainties in $\Delta \log L$ corresponding to parallax errors in the Hipparcos catalog, $\Delta \log T_{\text{eff}}$ of ± 0.01 dex ($\sim \pm 100$ K), and $\Delta [\text{Fe}/\text{H}]$ of ± 0.1 dex. The resulting mass value may also appreciably depend on the chosen set of theoretical evolutionary tracks (e.g., the systematic difference as large as $\sim 0.5 M_{\odot}$ for the case of metal-poor tracks between Lejeune & Schaerer (2001) and Girardi et al. (2000).; see also footnote 3 in Sato et al. 2008).

Table 2. Radial Velocities of 14 And

JD (-2450000)	Radial Velocity (m s ⁻¹)	Uncertainty (m s ⁻¹)
3005.9546	30.2	8.6
3245.2465	96.8	5.7
3332.0661	-106.7	4.0
3579.1759	45.6	6.2
3599.3078	104.9	9.3
3607.1357	127.2	6.6
3635.2106	68.1	6.2
3656.1741	-18.8	5.5
3693.0493	-93.2	4.3
3719.9577	-81.8	7.2
3726.0131	-1.1	7.0
3742.9362	-11.9	7.6
3775.9237	76.3	4.6
3938.2816	44.6	5.9
3962.2592	102.7	5.2
3975.1040	97.1	6.2
4018.0820	5.3	5.6
4049.1049	-52.6	5.5
4089.0127	-111.9	5.2
4104.8910	-38.6	7.3
4115.8872	-2.1	5.4
4142.9051	64.0	4.4
4219.2924	-70.8	4.6
4254.2487	-82.1	13.1
4305.1747	31.6	5.5
4338.1549	113.3	6.3
4349.1366	83.9	4.9
4378.1594	60.7	5.9
4384.0522	38.0	6.0
4415.9392	-55.8	5.0
4419.9316	-55.5	6.3
4460.0025	-92.7	10.1
4466.9496	-59.7	5.7
4491.8965	-4.1	7.6

Table 3. Orbital Parameters

Parameter	14 And	81 Cet	6 Lyn	HD 167042
P (days)	185.84±0.23	952.7±8.8	899±19	417.6±4.5
K_1 (m s ⁻¹)	100.0±1.3	62.8±1.5	36.2±1.7	33.3±1.6
e	0 (fixed)	0.206±0.029	0.134±0.052	0.101±0.066
ω (deg)	0 (fixed)	175.0±6.9	27±27	82±52
T_p (JD-2,450,000)	2861.4±1.5	2486±26	3309±60	2974±60
$a_1 \sin i$ (10 ⁻³ AU)	1.712±0.024	5.39±0.12	2.97±0.16	1.274±0.057
$f_1(m)$ (10 ⁻⁶ M_\odot)	1.936±0.079	2.30±0.15	0.431±0.062	0.158±0.022
$m_2 \sin i$ (M_J)	4.8	5.3	2.4	1.6
a (AU)	0.83	2.5	2.2	1.3
N_{obs}	34	33	30	29
rms (m s ⁻¹)	20.3	9.2	10.6	8.0
Reduced $\sqrt{\chi^2}$	3.3	1.7	1.6	1.5

Table 4. Radial Velocities of 81 Cet

JD (-2450000)	Radial Velocity (m s ⁻¹)	Uncertainty (m s ⁻¹)
2888.2622	56.6	6.5
2975.1133	46.7	8.2
3005.0714	41.2	4.3
3364.0728	-54.2	4.5
3403.9822	-72.0	5.1
3579.2561	-34.2	6.8
3599.3232	-15.9	7.5
3635.2973	-25.7	6.0
3659.2479	9.7	4.6
3693.1606	12.0	5.7
3727.0642	11.6	4.7
3743.0368	27.4	4.9
3774.9443	27.7	5.2
3811.9192	50.8	8.0
3938.3038	51.2	6.0
3963.2839	48.1	5.6
4018.1630	58.0	4.6
4051.1382	43.0	4.8
4089.0958	39.1	4.8
4127.9761	22.8	5.5
4142.9929	15.1	5.3
4147.9770	12.3	6.0
4170.9343	0.7	8.7
4171.9188	6.0	5.9
4305.2794	-52.2	6.4
4338.2888	-44.0	5.9
4349.2596	-58.3	5.8
4378.1919	-92.5	4.8
4416.0384	-70.6	4.8
4458.0891	-72.1	4.8
4467.0517	-59.0	4.7
4493.0207	-53.1	5.4
4526.9147	-28.9	5.1

Table 5. Radial Velocities of 6 Lyn

JD (-2450000)	Radial Velocity (m s ⁻¹)	Uncertainty (m s ⁻¹)
3028.2002	0.2	5.0
3107.9650	9.8	4.7
3290.2429	52.4	7.5
3307.1619	37.2	4.5
3363.3240	29.1	6.1
3448.0390	-15.3	6.3
3467.9581	-15.9	9.8
3494.9817	-0.8	10.3
3659.2879	-27.4	5.7
3694.3102	-24.2	6.2
3729.1980	-26.1	6.9
3743.1611	-25.2	6.2
3811.9435	-30.4	5.3
3852.9669	-3.6	7.1
4022.3010	29.4	6.2
4049.2443	16.4	7.7
4087.2793	38.8	6.0
4122.2054	42.1	5.5
4143.1678	50.4	7.2
4169.0485	29.1	5.5
4196.0062	19.2	7.9
4215.9689	41.8	6.3
4338.3163	-3.3	6.5
4379.2591	5.9	5.6
4416.1067	-4.0	7.0
4458.1686	-18.3	7.1
4492.1646	-42.8	5.6
4524.0101	-24.9	9.9
4553.9338	-32.8	5.2
4556.9840	-40.8	5.3

Table 6. Radial Velocities of HD 167042

JD (-2450000)	Radial Velocity (m s ⁻¹)	Uncertainty (m s ⁻¹)
3077.3248	-32.8	4.3
3161.1350	-14.7	5.2
3285.0198	13.1	4.3
3405.3778	-11.5	4.3
3499.1405	-32.0	5.6
3608.0945	2.0	5.9
3661.0231	21.0	5.1
3693.9118	40.8	8.1
3814.3203	4.9	5.2
3853.2342	-15.4	5.2
3889.2354	-38.4	8.8
3890.1815	-36.1	9.1
3948.1031	-13.4	6.4
3962.1760	-17.4	6.0
4018.0037	-8.7	5.0
4051.9409	8.6	5.6
4126.3613	29.7	5.8
4146.3220	39.9	5.5
4171.2461	29.4	5.0
4195.2715	26.0	5.5
4216.2184	13.5	5.0
4254.1603	-9.9	5.9
4305.0598	-25.2	7.0
4338.0740	-35.6	5.3
4379.0062	-33.2	5.0
4417.8831	-13.4	5.5
4495.3581	35.8	6.5
4524.3108	34.3	4.9
4554.3268	39.9	5.4

Table 7. Bisector Quantities

Bisector Quantities	14 And	81 Cet	6 Lyn	HD 167042
Bisector Velocity Span (BVS) (m s^{-1})	19.8 ± 5.8	2.4 ± 3.0	-5.5 ± 5.1	1.0 ± 4.3
Bisector Velocity Curve (BVC) (m s^{-1})	-1.6 ± 2.8	-2.8 ± 2.1	-0.3 ± 4.1	1.9 ± 3.1
Bisector Velocity Displacement (BVD) (m s^{-1})	-177.0 ± 11.2	-115.3 ± 7.4	-60.9 ± 8.9	-58.9 ± 8.0